

Ab-initio study of structural, elastic, electronic and thermodynamic properties of $\text{Ba}_x\text{Sr}_{1-x}\text{S}$ ternary alloys

S. CHELLI¹, S. TOUAM¹, L. HAMIoud¹, H. MERADJI^{1*}, S. GHEMID¹, F. EL HAJ HASSAN²

¹Laboratoire LPR, Département de Physique, Faculté des Sciences, Université Badji Mokhtar, Annaba, Algeria

²Laboratoire de Physique et d'électronique (LPE), Faculté des Sciences, Université Libanaise, El Hadath, Beirut, Lebanon

The structural, elastic, electronic and thermodynamic properties of $\text{Ba}_x\text{Sr}_{1-x}\text{S}$ ternary alloys have been investigated using the full-potential (linearized) augmented plane wave method. The ground state properties, such as lattice constant, bulk modulus and elastic constants, are in good agreement with numerous experimental and theoretical data. The dependence of the lattice parameters, bulk modulus and band gap on the composition x was analyzed. Deviation of the lattice constant from Vegard's law and the bulk modulus from linear concentration dependence (LCD) was observed. The microscopic origins of the gap bowing were explained by using the approach of Zunger et al. The thermodynamic stability of $\text{Ba}_x\text{Sr}_{1-x}\text{S}$ alloy was investigated by calculating the excess enthalpy of mixing, ΔH_m and the calculated phase diagram showed a broad miscibility gap with a critical temperature.

Keywords: *ternary alloys; first principle calculations; elastic constants; thermodynamic properties*

© Wrocław University of Technology.

1. Introduction

Computer simulations allow the investigation of many materials properties and processes that are not easily accessible in a laboratory. This is particularly true in the earth sciences, where the relevant pressures and temperatures may be so extreme that no experimental techniques can operate at those conditions. Many computer simulations are performed using effective inter-atomic potentials tailored to reproduce some experimentally observed properties of the materials being investigated. First-principles techniques based on density-functional theory (DFT) [1, 2] are much more predictive, not biased by any prior experimental input, and have demonstrated a considerable accuracy in a wide class of materials and variety of external conditions.

Alkaline-earth chalcogenides belonging to the binary group II – VI have recently attracted great attention of researchers because of their

potential use as thermionic photoluminescent, phosphorescent, cathodoluminescent and other optoelectronic materials [3–5]. BaS and SrS, two alkaline earth sulfide members of the same group have proven to be excellent phosphor host materials and, since recently, are considered to be of great use in the display and optoelectronic devices [6]. These compounds are technically very important having applications ranging from catalysis to microelectronics [7]. A number of theoretical works exist in the literature dealing with structural, electronic, elastic and thermodynamic properties of SrS and BaS. Specifically, Tuncel et al. [8] reported the structural, elastic, vibrational and thermodynamic properties of BaX ($X = \text{S}, \text{Se}$ and Te) using density functional theory (DFT) method. The structural, elastic, and electronic properties of barium chalcogenides have been studied by Bouhemadou et al. [9]. Using the full potential linearized augmented plane wave (FP-LAPW) method, Pourghazi et al. [10] calculated the reflectivity and imaginary part of the dielectric function for BaSe, BaS and BaTe. First

*E-mail: hmeradji@yahoo.fr

principle calculations of structural, electronic and thermodynamic properties of SrS have been carried out by Labidi *et al.* [11]. Using density-functional perturbation theory, the lattice dynamics of SrX ($X = S, Se$ and Te) and their pressure dependence in both B1 (NaCl structure) and B2 (CsCl structure) phases have been investigated by Souadkia *et al.* [12]. The structural and electronic properties of BaS and SrS binary compounds were investigated in previous experimental [13–15] studies. However, the thermodynamic properties of these materials are rarely studied.

Usually, the thermodynamic properties of materials are the basis of solid state science and industrial applications. Furthermore, the study of the thermodynamic properties of materials is of importance to extend our knowledge on their specific behavior when undergoing severe constraints of high-pressure and high temperature environments. This is particularly true since the emergence of modern technologies (geophysics, astrophysics, particle accelerators, fission and fusion reactors, etc.), from which we always expect new advances and innovations in material science to reach higher performances.

With the motivation of finding promising ternary alloys from these binary compounds with improved physical properties in comparison with other ternary alloys, the present study focuses mainly on the composition dependence of the structural, electronic, elastic and thermodynamic properties of $Ba_xSr_{1-x}S$ ternary alloys by performing *ab initio* calculations, based on the full-potential linearized augmented plane wave method (FP-LAPW) within density functional theory as implemented in the WIEN2k code [16]. The paper has been divided into three parts. In section 2, we briefly describe the computational technique used in this study. The most relevant results obtained for the structural, electronic, elastic, thermal and thermodynamic properties of SrS, BaS and $Ba_xSr_{1-x}S$ ternary alloys are presented and discussed in section 3. Finally, in section 4, we summarize the main conclusions of our work.

2. Calculation method

The calculations were carried out using the full potential linearized plane wave (FP-LAPW) method within a framework of density functional theory (DFT) as implemented in WIEN2k code. For the exchange correlation potential, we have used the Perdew-Burke-Ernzerhof generalized gradient approximation (PBE-GGA) [17]. In addition, the recent Tran and Blaha-modified Becke-Johnson potential (mBJ) [18] was also used for the electronic properties to avoid the well-known GGA underestimation of the band gap. In the FP-LAPW method, the wave functions are expanded in a linear combination of radial functions times spherical harmonics inside non-overlapping muffin-tin spheres of radius R_{MT} surrounding each atom and in plane waves in the interstitial region between the spheres. The muffin-tin radii were taken as 2.5, 2.1 and 2.2 a.u. for Ba, S and Sr, respectively. A plane wave cut-off $R_{MT} \cdot K_{max} = 8$ (where R_{MT} is the smallest of all MT sphere radii and K_{max} is the maximum value of the wave vector K) was chosen for the expansion of the wave functions in the interstitial region. The maximum l for the expansion of the wave function in spherical harmonics inside the muffin tin spheres was taken to be $l_{max} = 10$.

3. Results

3.1. Structural properties

The first step in any *ab initio* calculation is to find the optimized geometry of the crystalline structure. For the studied materials we used eight-atom simple cubic cells. The lattice structures have been modeled at some selected compositions $x = 0.25, 0.5$, and 0.75 . For each composition, we carried out a structural optimization by minimizing the total energy with respect to the cell volume and also the atomic positions. The total energy has been calculated as a function of unit cell volume and was fitted to the Murnaghan's equation of state [19]. This allowed obtaining the equilibrium structural properties, such as the lattice constant (a) and the bulk modulus (B). Table 1 summarizes the results of our calculations and

compares them with other experimental and theoretical predictions. Considering the general trend that GGA usually overestimates the lattice parameters, our PBE-GGA results for SrS and BaS are in good agreement with the experimental and theoretical values. For the compositions $x = 0.25, 0.5$ and 0.75 , our results are in reasonable agreement with those of Ameri et al. [23] using FP-LMTO method. The small differences are related to the parameters used in both methods.

The calculated lattice constants for different alloy concentrations follow the Vegard's Law [29] with a slight upward bowing parameter equal to -0.066 \AA obtained by fitting the calculated values with a polynomial function (Fig. 1). This fact suggests that there is a good agreement between the DFT predictions and the linear Vegard's law. The lattice parameter increases with increasing Ba composition because the atom of Sr is smaller than that of Ba.

The overall behavior of the variation of the bulk modulus as a function of the composition for the $Ba_xSr_{1-x}S$ alloys is presented in Fig. 2, and compared to the results predicted by linear concentration dependence (LCD). A weak deviation from the LCD is observed with the downward bowing equal to 1.909 GPa . This might be mainly due to the weak mismatch between the bulk modulus of the binary compounds constituting the alloy.

3.2. Elastic properties

The elastic constants of solids provide a link between the mechanical and dynamic behaviors of crystals and provide important information concerning the nature of the forces operating in solids.

In particular, they provide information on the stability and stiffness of materials. The elastic constants C_{ij} are obtained by calculating the total energy as a function of volume conserving strains that break the symmetry, using the method developed by Charpin and integrated in the WIEN2k code [16]. For the cubic crystal, there are only three independent elastic constants: C_{11} , C_{12} and C_{44} . A set of three equations is needed to determine all the constants. This means that three types of strain must be applied to the starting crystal.

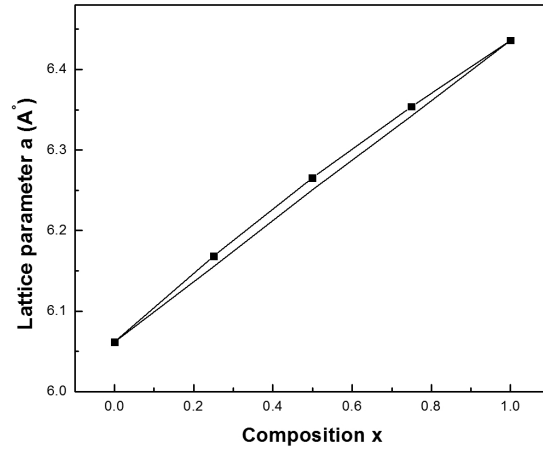


Fig. 1. Composition dependence of the calculated lattice constants (solid squares) of $Ba_xSr_{1-x}S$ alloys compared with Vegard's prediction (solid line).

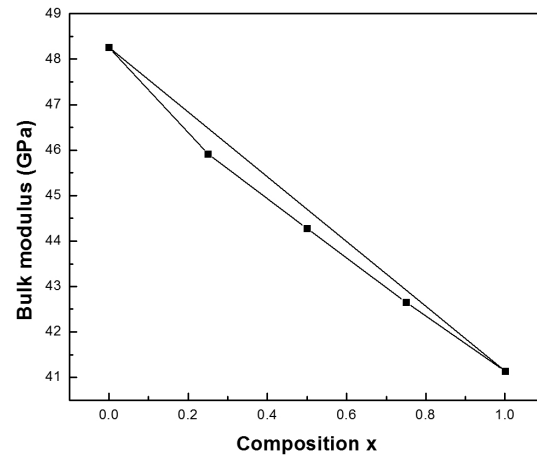


Fig. 2. Composition dependence of the calculated bulk modulus (solid squares) of $Ba_xSr_{1-x}S$ alloys compared with the predicted linear composition dependence (solid line).

The first type involves calculating the bulk modulus B which is related to the elastic constants by $B = (C_{11} + 2C_{12})/3$. The second type, which permits to obtain $C_{11} - C_{12}$, involves performing volume-conserving tetragonal strains. The last type of deformation, which yields $C_{11} + 2C_{12} + 4C_{44}$, is a rhombohedral distortion. The calculated PBE-GGA elastic constants for the $Ba_xSr_{1-x}S$ ternary

Table 1. Calculated lattice constant a , bulk modulus B and its pressure derivative B' for the $Ba_xSr_{1-x}S$ alloys, compared with available experimental measurements data and previous theoretical calculations.

$Ba_xSr_{1-x}S$ ($0 \leq x \leq 1$)	Present work PBE-GGA	Experiments	Other calculations
SrS			
$a(\text{\AA})$	6.061	6.024 ^a	6.064 ^b , 5.972 ^b , 5.774 ^c , 6.023 ^e , 6.05 ^f , 6.076 ^{d,g} , 6.065 ^h
$B(\text{GPa})$	48.25	58 ^a	48.24 ^d , 47.94 ^b , 62 ^c , 51.103 ^e , 48.30 ^f , 47 ^g , 46.263 ^h
B'	4.358		4.34 ^b , 4.19 ^g
Ba_{0.25}Sr_{0.75}S			
$a(\text{\AA})$	6.168		6.119 ^e
$B(\text{GPa})$	45.91		57.271 ^e
B'	4.589		
Ba_{0.5}Sr_{0.5}S			
$a(\text{\AA})$	6.266		6.208 ^e
$B(\text{GPa})$	44.28		55.215 ^e
B'	4.340		
Ba_{0.75}Sr_{0.25}S			
$a(\text{\AA})$	6.353		6.310 ^e
$B(\text{GPa})$	42.65		49.341 ^e
B'	4.346		
BaS			
$a(\text{\AA})$	6.436	6.38 ⁱ	6.41 ^e , 6.469 ^j , 6.444 ^k , 6.44 ^l , 6.446 ^m , 6.27 ⁿ , 6.407 ^o
$B(\text{GPa})$	41.14	39.42 ⁱ	37.299 ^e , 42.36 ^j , 40.93 ^l , 40.28 ^m , 52.39 ⁿ
B'	4.194		5.81 ^j , 4.92 ⁿ

^a[13], ^b[20], ^c[21], ^d[22], ^e[23], ^f[12], ^g[7], ^h[11], ⁱ[24], ^j[9], ^k[25], ^l[26], ^m[27], ⁿ[8], ^o[28]

alloys are listed in Table 2. The requirement of mechanical stability in a cubic structure leads to the following restrictions on the elastic constants: $C_{11} - C_{12} > 0$, $C_{11} + 2C_{12} > 0$, $C_{11} > 0$, $C_{44} > 0$ and $C_{12} < B < C_{11}$.

For each composition x , these criteria are satisfied, indicating that these compounds are elastically stable. For the binary compounds SrS and BaS, the obtained elastic constants values agree with those given in other theoretical works, hence, it is reasonable to expect that elastic constants of the alloys can be described with similar accuracy in our calculations. On the other hand, the relation $B = (C_{11} + 2C_{12})/3$ provides a useful internal consistency check between the various computational procedures. As Table 2 shows, the bulk modulus values calculated using this relation agree well with those obtained from the total energy fitting to

Murnaghan's equation of state. One can remark that C_{44} , which reflects the resistance to shear deformation, is lower than C_{11} , which is related to the unidirectional compression along the principal crystallographic directions, which means that the cubic cell is more easily deformed by a shear in comparison to the unidirectional compression.

3.3. Electronic properties

We have calculated the band structures for the $Ba_xSr_{1-x}S$ alloys along the high directions in the first Brillouin zone at the calculated equilibrium lattice constants. The calculated band gaps for all studied compositions ($x = 0, 0.25, 0.50, 0.75, 1$) are given in Table 3, along with the available experimental and theoretical results. It is clear that for the binary compounds SrS and BaS, the band gap values given by the mBJ scheme are in

Table 2. Calculated elastic constants C_{ij} (in GPa) for the $Ba_xSr_{1-x}S$ alloys compared with other theoretical works.

	This work	Other calculations
SrS		
C_{11}	100.4	141 ^a , 113.9 ^b , 130.1 ^c
C_{12}	15.75	17.2 ^a , 19.4 ^b
C_{44}	26.88	62.5 ^a , 30.3 ^b , 49.8 ^c
B^*	43.96	
$Ba_{0.25}Sr_{0.75}S$		
C_{11}	107.5	
C_{12}	17.93	
C_{44}	24.82	
B^*	47.78	
$Ba_{0.5}Sr_{0.5}S$		
C_{11}	96.48	
C_{12}	20.77	
C_{44}	20.68	
B^*	46.00	
$Ba_{0.75}Sr_{0.25}S$		
C_{11}	95.65	
C_{12}	17.76	
C_{44}	21.00	
B^*	43.72	
BaS		
C_{11}	80.14	115 ^d , 94.57 ^e , 86.80 ^f , 107.48 ^g
C_{12}	24.51	17 ^d , 19.61 ^e , 16.90 ^f , 24.83 ^g
C_{44}	18.30	18 ^d , 18.60 ^e , 31.60 ^f , 30.26 ^g
B^*	43.05	

^a[7], ^b[30], ^c[31], ^d[9], ^e[32], ^f[33], ^g[8]

$$B^* = (C_{11} - 2C_{12})/3$$

better agreement with the available experimental results in comparison with the values calculated by PBE-GGA. The modified Becke-Johnson potential (mBJ) as proposed by Tran and Blaha reproduces very well the step structure of the exact exchange potential, which is an important result because only the semi local quantities are used [41]. The agreement with experiment is very good for solids and it is of the same order as the agreement obtained with the hybrid functionals or the GW methods. Fig. 3 shows the composition dependence of the calculated band gaps using PBE-GGA and mBJ schemes. The band gap decreases non-linearly

with increasing of Ba content. We calculated the total bowing parameter by fitting the non-linear variation of calculated band gaps versus concentration with quadratic function. The results obey the following variations:

$$E_g^{PBE-GGA}(x) = 2.517 - 0.515x + 0.248x^2 \quad (1)$$

$$E_g^{mBJ}(x) = 3.644 - 0.628x + 0.356x^2 \quad (2)$$

The quadratic terms in equation 1 and equation 2 are referred to be the band gap bowing parameters.

Table 3. Band-gap energies (in eV) of $\text{Ba}_x\text{Sr}_{1-x}\text{S}$ alloys at various concentrations x .

Alloy	x	This work		Experiments	Other calculations
		mBJ	PBE-GGA		
$\text{Ba}_x\text{Sr}_{1-x}\text{S}$	0	3.663	2.535	4.32 ^a	2.15 ^b , 2.53 ^c , 2.30 ^d , 2.29 ^e , 2.45 ^f
	0.25	3.469	2.365		2.316 ^e
	0.5	3.426	2.331		2.316 ^e
	0.75	3.404	2.297		2.316 ^e
	1	3.356	2.235	3.88 ^g , 3.9 ^h	2.084 ^e , 2.26 ⁱ , 2.17 ^j , 3.07 ^k , 2.30 ^l

^a[34], ^b[35], ^c[11], ^d[36], ^e[23], ^f[37], ^g[38], ^h[39], ⁱ[9], ^j[28], ^k[9], ^l[40]

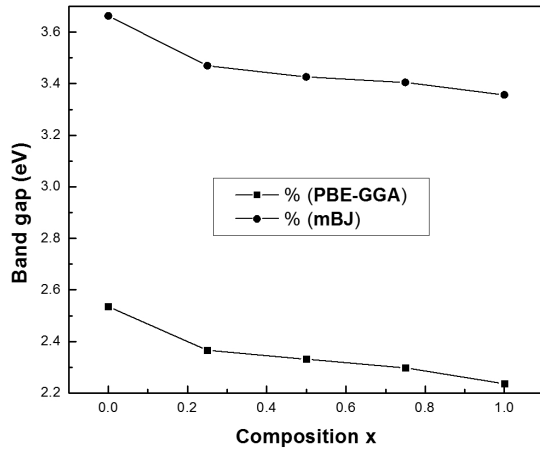


Fig. 3. Composition dependence of the calculated band gap using PBE-GGA and mBJ approximations for $\text{Ba}_x\text{Sr}_{1-x}\text{S}$ alloys.

To analyze the physical origins of the band gap bowing, we followed the procedure of Bernard and Zunger [42] and decomposed the bowing parameter into three physically distinct contributions:

$$b = b_{VD} + b_{CE} + b_{SR} \quad (3)$$

The effect of volume deformation causes the first term of the bowing parameter, b_{VD} in equation 3. The notional response of SrS (BaS) to hydrostatic pressure describes this term via the effect of the contribution of balanced lattice constant a_{SrS} (a_{BaS}) in relation to the lattice constant of the alloy value $a(x)$:

$$b_{VD} = 2[\epsilon_{\text{SrS}}(a_{\text{SrS}}) - \epsilon_{\text{SrS}}(a) + \epsilon_{\text{BaS}}(a_{\text{BaS}}) - \epsilon_{\text{BaS}}(a)] \quad (4)$$

The charge transfer in SrS and BaS at $a = a(x)$ indicates the second term, b_{CE} , of the total band gap bowing parameter:

$$b_{CE} = 2[\epsilon_{\text{SrS}}(a) + \epsilon_{\text{BaS}}(a) - 2\epsilon_{\text{BaSrS}}(a)] \quad (5)$$

The third term, b_{SR} refers to the structural relaxation which measures the changes in passing from the unrelaxed to the relaxed alloy:

$$b_{SR} = 4[\epsilon_{\text{BaSrS}}(a) - \epsilon_{\text{BaSrS}}(a_{eq})] \quad (6)$$

ϵ is the energy gap which has been calculated for the indicated atomic structures and lattice constants. The calculated gap bowing contributions of the band gap are presented in Table 4. We note that the calculated quadratic parameters of the gap bowing are very close to those calculated using Zunger approach. The charge transfer contribution b_{CE} dominates the total gap bowing parameter in the $\text{Ba}_x\text{Sr}_{1-x}\text{S}$ alloy, which is related to electronegativity mismatch between the constituting atoms: Ba(0.89), Sr(0.95) and S(2.52).

3.4. Thermodynamic properties

In this part, we investigate the phase stability of ternary alloys $\text{Ba}_x\text{Sr}_{1-x}\text{S}$. At finite temperature, the thermodynamic stability of a solid system can be determined by Gibbs free energy model as detailed in references [43, 44].

Using this approach, the Gibbs free energy is calculated using the following expression:

$$\Delta G_m = \Delta H_m - T \Delta S_m \quad (7)$$

where

$$\Delta H_m = \Omega x(1-x) \quad (8)$$

Table 4. Decomposition of the bowing parameter into volume deformation (VD), charge exchange (CE) and structural relaxation (SR) contributions, compared with the typical bowing obtained by a quadratic fit.

Alloy	x	Zunger approach		Quadratic fit	
		mBJ	PBE-GGA	mBJ	PBE-GGA
$Ba_xSr_{1-x}S$	b_{VD}	0.014	-0.029		
	b_{CE}	0.375	0.300		
	b_{SR}	-0.056	-0.052		
	b	0.333	0.218	0.356	0.248

$$\Delta S_m = -R[x \ln x + (1-x) \ln 1-x] \quad (9)$$

ΔH_m and ΔS_m are the enthalpy and entropy of mixing, respectively, Ω is the interaction parameter which depends on the material, R is the gas constant, and T is the absolute temperature. The mixing enthalpy of alloys can be obtained as the difference in energy between the alloy and the weighted sum of the constituents:

$$\Delta H_m = E_{AB_xC_{1-x}} - xE_{AB} - (1-x)E_{AC} \quad (10)$$

where $E_{AB_xC_{1-x}}$, E_{AB} and E_{AC} are the respective energies of AB_xC_{1-x} alloy and the binary compounds AB and AC. By rewriting expression 8 as $\Omega = \Delta H_m / x(1-x)$, we can calculate, for each x , a value of Ω from the above DFT values of ΔH_m . The interaction parameter increases almost linearly with increasing x . By a linear fit we obtained:

$$\Omega \text{ (Kcal/mol)} = 3.131 - 0.506x \quad (11)$$

The average value of x -dependent Ω in the range of $0 \leq x \leq 1$ derived from this equation for $Ba_xSr_{1-x}S$ alloy is 2.878 Kcal/mol. By calculating the free energy of mixing ΔG_m at different concentrations using equations 7 to 9, we can determine the T - x phase diagram which shows the stable, metastable, and unstable mixing regions of the alloy. At a temperature lower than the critical temperature T_c , the two binodal points are determined as those points at which the common tangent line approaches the ΔG_m curves. The two spinodal points are determined as those points at which the second derivative of ΔG_m is zero; $\partial^2(\Delta G_m)/\partial x^2 = 0$.

Fig. 4 shows the calculated phase diagram including the spinodal and binodal curves for the alloy of interest. We observed a critical temperature T_c of 702 K for $Ba_xSr_{1-x}S$. We have calculated the phase diagram by using the average value of the x -dependent Ω , hence, the phase diagram looks symmetric. The spinodal curve in the phase diagram marks the equilibrium solubility limit, i.e. the miscibility gap. For temperatures and compositions above this curve, a homogeneous alloy is predicted. The wide range between the spinodal and binodal curves indicates that the alloy may exist as a metastable phase. Hence, our results indicate that the alloy $Ba_xSr_{1-x}S$ is stable at high temperature.

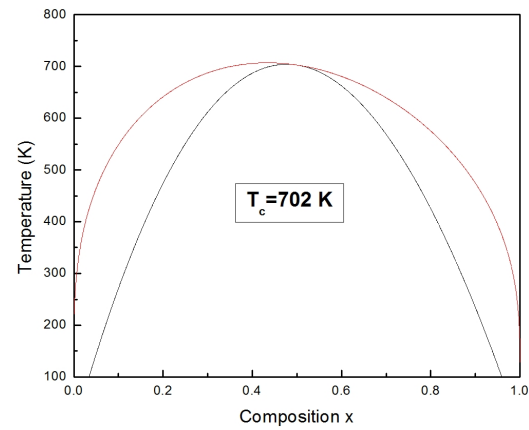


Fig. 4. T - x phase diagram for $Ba_xSr_{1-x}S$ alloys. Reddish line: binodal curve; gray line: spinodal curve.

4. Conclusion

In summary, using the FP-LAPW method, we have investigated the structural, elastic, electronic and thermodynamic properties of $Ba_xSr_{1-x}S$ alloys. Our main results are as follows:

- The calculated lattice constants and bulk modulus for the binary compounds (SrS and BaS) are in reasonable agreement with the experimental data and previous theoretical results; this might be a confirmation of the reliability and accuracy of the predicted lattice parameters for the studied ternary alloys.
- The elastic constants have been predicted.

(iii) The gap bowing is mainly caused by the charge-transfer effect, while the contribution of volume deformation and the structural relaxation is less important.

(iv) The calculated phase diagram indicates that the $\text{Ba}_x\text{Sr}_{1-x}\text{S}$ is stable at high temperature.

References

- [1] HOHENBERG P., KOHN W., *Phys. Rev. B*, 136 (1964), 864.
- [2] KOHN W., SHAM L.J., *Phys. Rev. A*, 140 (1965), 1133.
- [3] PANDEY R., *Mater. Sci.*, 5 (1986), 3357.
- [4] ASANO S., YAMASHITA N., NAKAO Y., *Phys. Status Solidi*, 89 (1978) 663.
- [5] NAKANISHI Y., LTO T., HATANAKA Y., SHI-MAOKA G., *Appl. Surf. Sci.*, 66 (1992), 515.
- [6] YAMASHITA N., *J. Phys. Soc. Jpn.*, 30 (1991), 3335.
- [7] KHENATA R., BALTACHE H., RÉAT M., DRIZ M., SAHNOUN M., BOUHAFFS B., ABBAR B., *Physica B*, 339 (2003), 208.
- [8] TUNCEL E., COLAKOGLU K., DELIGOZ E., CIFTCI Y.O., *J. Phys. Chem. Solids*, 70 (2009), 371.
- [9] BOUHEMADOU A., KHENATA R., ZEGRAR F., SAHNOUN M., BALTACHE H., RESHAK A.H., *Comp. Mater. Sci.*, 38 (2006), 263.
- [10] POURGHAZI A., DADSETANI M., *Physica B*, 370 (2005), 35.
- [11] LABIDI S., MERADJI H., LABIDI M., GHEMID S., DRABLIA S., EL HAJ HASSAN F., *Phys Procedia*, 2 (2009), 1205.
- [12] SOUADKIA M., BENNECER B., KALARASSE F., MEL-LOUKI A., *Comp. Mater. Sci.*, 50 (2011), 1701.
- [13] SYASSEN K., *Phys. Status Solidi A*, 91 (1985), 11.
- [14] ZHANG S., LI H., ZHOU S., CAO X., *J. Phys. Chem. B*, 111 (2007), 1304.
- [15] KALPANA G., PALANIVEL B., RAJAGOPALAN M., *Phys. Rev. B*, 50 (1994), 12318.
- [16] BLAHA P., SCHWARZ K., MADSEN G.K.H., KVAS-NICKA D., LUITZ J., *WIEN2K, An Augmented Plane Wave Plus Local Orbitals Program For Calculating Crystal Properties*, Karlheinz Schwars, Techn. Universitat, Wien, 2001.
- [17] PERDEW J.P., BURKE K., ERNZERHOF M., *Phys. Rev. Lett.*, 77 (1996), 3865.
- [18] TRAN F., BLAHA P., *Phys. Rev. Lett.*, 102 (2009), 226401.
- [19] MURNAGHAN F.D., *P. Natl. Acad. Sci. USA*, 30 (1944), 5390.
- [20] SHAUKAT A., SAEED Y., NAZIR S., IKRAM N., TAN-VEEN M., *Physica B*, 404 (2009), 3964.
- [21] CHEN Z.J., XIAO H.Y., ZUA X.T., *Physica B*, 391 (2007), 193.
- [22] XIAO-CUI Y., AI-MIN H., JIE Y., YONG-HAO H., GANG P., CHUN-XIAO G., GUANG-TIAN Z., *Chinese Phys. Lett.*, 25 (2008), 1807.
- [23] AMERI M., BOUDIA K., RABHI A., BENAÏSSA S., AL-DOURI Y., RAIS A., HACHEMANE D., *Mater. Sci. Appl.*, 3 (2012), 861.
- [24] YAMAOKA S., SHIMOMURO O., NAKAZAWA H., FUKUNAGA O., *Solid State Commun.*, 33 (1980), 87.
- [25] FENG Z., HU H., CUI S., WANG W.J., *Physica B*, 404 (2009), 2107.
- [26] DRABLIA S., MERADJI H., GHEMID S., NOUET G., EL HAJ HASSAN F., *Comp. Mater. Sci.*, 46 (2009), 376.
- [27] EL HAJ HASSAN F., AKBARZADEH H., *Comp. Mater. Sci.*, 38 (2006), 362.
- [28] LIN G.Q., GONG H., WU P., *Phys. Rev. B*, 71 (2005), 85203.
- [29] VEGARD L., *Z. Phys. Chem.*, 5 (1921), 17.
- [30] CHENG Y., LU L.-Y., JIA O.-H., GOU Q.-Q., *Commun. Theor. Phys.*, 49 (2008), 1611.
- [31] BHARDWAJ P., SINGH S., *Measurement*, 46 (2013), 1161.
- [32] GÖKOĞLU G., *J. Phys. Chem. Solids*, 69 (2008), 2924.
- [33] ABO-HASSAN K.M.M., MUHAMAD M.R., RAD-HAKRISHNA S., *Thin Solid Films*, 491 (2005), 117.
- [34] KANEKO Y., KODA T., *J. Cryst. Growth*, 86 (1988), 72.
- [35] SHAUKAT A., SAEED Y., NAZIR S., IKRAM N., TAN-VEEN M., *Physica B*, 404 (2009), 3964.
- [36] CHARIFI Z., BAAZIZ H., EL HAJ HASSAN F., BOUARISSA N., *J. Phys.-Condens. Mat.*, 17 (2005), 4083.
- [37] BACHELET G.B., CHRISTENSEN N.E., *Phys. Rev. B*, 31 (1985), 879.
- [38] ZOLWEG R.J., *Phys. Rev.*, 11 (1958), 113.
- [39] KANEKO Y., MORIMOTO K., KODA T., *J. Ceram. Soc. Jpn.*, 52 (1985), 4385.
- [40] KALPANA G., PALANIVEL B., RAJAGOPALAN M., *Phys. Rev. B*, 50 (1994), 12318.
- [41] SINGH H., SINGH M., KUMAR S., KASHYAP M.K., *Physica B*, 406 (2011), 3825.
- [42] BERNARD J.E., ZUNGER A., *Phys. Rev. Lett.*, 34 (1986), 5992.
- [43] SWALIN R.A., *Thermodynamics of Solids*, Wiley, New York, 1972.
- [44] TELES L.K., FURTHMULLER J., SCOLFARO L.M.R., LEITE J.R., BECHSTEDT F., *Phys. Rev. B*, 62 (2000), 2475.

Received 2015-04-08

Accepted 2015-09-08